Aalborg Universitet

AALBORG UNIVERSITY
DENMARK

Enhanced Phase-Shifted Current Control for Harmonic Cancellation in Three-Phase Multiple Adjustable Speed Drive Systems

Yang, Yongheng; Davari, Pooya; Zare, Firuz; Blaabjerg, Frede

Published in:
I E E E Transactions on Power Delivery

DOI (link to publication from Publisher):
10.1109/TPWRD.2016.2590570

Publication date:
2017

Document Version
Accepted author manuscript, peer reviewed version

Link to publication from Aalborg University

Citation for published version (APA):
Yang, Y., Davari, P., Zare, F., & Blaabjerg, F. (2017). Enhanced Phase-Shifted Current Control for Harmonic Cancellation in Three-Phase Multiple Adjustable Speed Drive Systems. *I E E E Transactions on Power Delivery*, *32*(2), 996-1004. https://doi.org/10.1109/TPWRD.2016.2590570

General rights
Copyright and moral rights for the publications made accessible in the public portal are retained by the authors and/or other copyright owners and it is a condition of accessing publications that users recognise and abide by the legal requirements associated with these rights.

- Users may download and print one copy of any publication from the public portal for the purpose of private study or research.
- You may not further distribute the material or use it for any profit-making activity or commercial gain
- You may freely distribute the URL identifying the publication in the public portal -

Take down policy
If you believe that this document breaches copyright please contact us at vbn@aub.aau.dk providing details, and we will remove access to the work immediately and investigate your claim.

Enhanced Phase-Shifted Current Control for Harmonic Cancellation in Three-Phase Multiple Adjustable Speed Drive Systems

Yongheng Yang, *Member, IEEE,* Pooya Davari, *Member, IEEE,* Firuz Zare, *Senior Member, IEEE,* and Frede Blaabjerg, *Fellow, IEEE*

***Abstract*—A phase-shifted current control can be employed to mitigate certain harmonics induced by the Diode Rectifiers (DR) and Silicon-Controlled Rectifiers (SCR) as the front-ends of multiple parallel Adjustable Speed Drive (ASD) systems. However, the effectiveness of the phase-shifted control relies on the loading condition of each drive unit as well as the number of drives in parallel. In order to enhance the harmonic cancellation by means of the phase-shifted current control, the currents drawn by the rectifiers should be maintained almost at the same level. Thus, this paper firstly analyzes the impact of unequal loading among the parallel drives, and a scheme to enhance the performance is introduced to improve the quality of the total grid current, where partial loading operation should be enabled. Simulation and experimental case studies on multi-drive systems have demonstrated that the enhanced phase-shifted current control is a cost-effective solution to multiple ASD systems in terms of harmonic cancellation.**

***Index Terms*—Harmonics, phase-shifted current control, Diode Rectifiers (DR), Silicon-Controlled Rectifiers (SCR), three-phase multiple drives, adjustable speed drives.**

I. Introduction

HARMONICS and efficiency are always major issues for industrial drives, including Adjustable Speed Drive (ASD) systems [1]–[5]. At present, a lot of three-phase ASD drives still employ 6-pulse-bridge "uncontrollable" Diode Rectifier (DR) or "half-controllable" Silicon-Controlled Rectifiers (SCR) as the front-ends [1], [6], [7], mainly because of their low cost, simple control structure, and high reliability during operation. Fig. 1 then exemplifies a two-drive system consisting of a DR-fed and a SCR-fed drive. Basically, the major responsibility of the front-end apparatuses is to convert the alternative-current (ac) power to the direct-current (dc) power that is used by the Variable-Frequency Converter (VFC). However, this ac-dc rectification also brings significant harmonic currents that distort the modern power grid, leading to poor power quality. The harmonic currents appearing in the grid can potentially: 1) trigger system resonance, 2) lower the energy conversion efficiency, and 3) cause malfunctions of the equipment that is also connected to the Point of Common Coupling (PCC) [8]. Hence, regulations concerning harmonic

Manuscript received December 15, 2015; revised May 19, 2016; accepted July 09, 2016. Paper no. TPWRD-01805-2015.

Y. Yang, P. Davari, and F. Blaabjerg are with the Department of Energy Technology, Aalborg University, Aalborg DK-9220, Denmark (e-mail: yoy@et.aau.dk; pda@et.aau.dk; fbl@et.aau.dk).

F. Zare is with the Power and Energy Group, The University of Queensland, St. Lucia QLD 4072, Australia (e-mail: f.zare@uq.edu.au).

Color versions of one or more of the figures in this paper are available online at http://ieeexplore.ieee.org

Digital Object Identifier 10.1109/TPWRD.2016.2590570

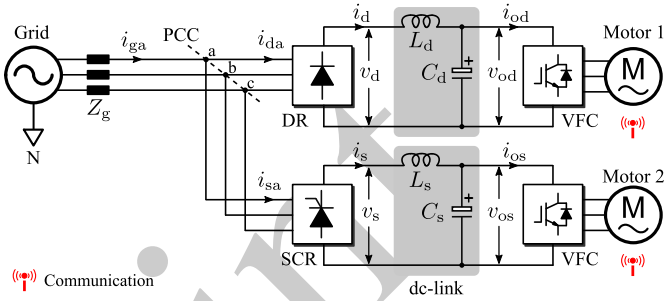

Fig. 1. Schematic of a two-drive system consisting of a SCR and a DR, where communication between the drives is also possible.

emissions by the drive systems are released and are also continuously updated [9], [10].

At the same time, state-of-the-art strategies are also developed to address this harmonic issue in motor drive applications [1], [5], [11], [12], which can simply be categorized into four types, depending on the schemes that have been used. As the simplest and the most straightforward way, passive devices like ac and dc chokes can be installed [5], [13], [14]. However, large in size, heavy in weight, and high potentials of resonance have hindered its extensive applications, especially in high power drives. Alternatively, the use of phase-shifting transformers as the very front-ends can increase the pulse number of the ac-dc rectifiers [15]–[21], which in return will significantly alleviate the distortion level at the grid side [22]. For instance, in [15], a 12-pulse rectifier front-end has been formed with a multi-pulse transformer and auxiliary circuits, which results in a Total Harmonic Distortion (THD) level of the grid current being lower than 6% in a wide range of loading levels. While in [20], an 18-pulse rectifier system has been presented, leading to even lower THDs. Nevertheless, the cost and overall volume of phase-shifting transformers are the major drawbacks [18]. In addition, the active power filtering techniques can be employed [7], [23]–[26]. The active power filtering techniques seem as promising solutions in terms of the effectiveness in harmonic mitigation, while at the cost of overall control complexity. Such techniques are more suitable in low-power applications [27]. Furthermore, there are hybrid harmonic mitigation solutions reported in literature [21], [27], [28]. In all, either increased system overall volume and/or the control complexity can be observed in the above applications, being a big barrier for size- and cost-effective ASD systems, which however is still of high interest.

Additionally, as it has been emphasized in [1], [11], the harmonic controllability or the harmonic mitigation flexibility

Post-Print

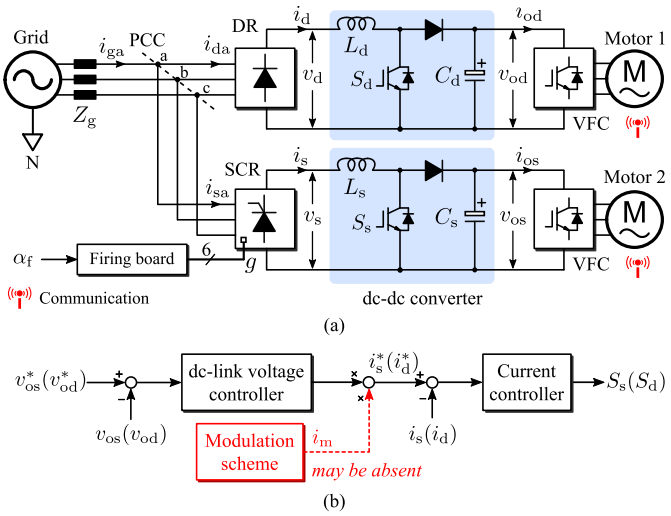

Fig. 2. A two-drive system consisting of a SCR and a DR, where boost dc-dc converters have been employed in the dc-links and $i_{\rm m}$ is the modulation signal: (a) hardware schematic and (b) overall dc-link control structure.

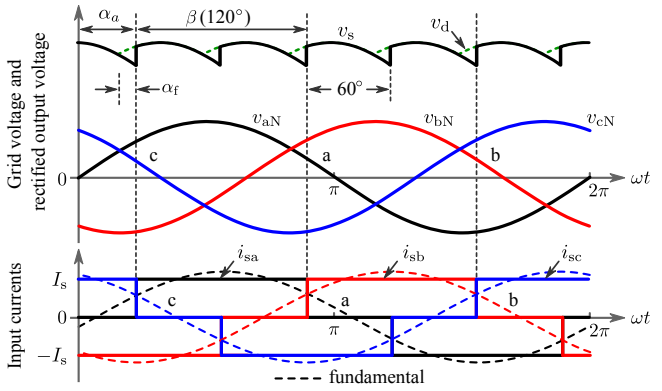

Fig. 3. Typical dc-link voltage, grid voltage and grid current waveforms of a SCR-fed drive system, where the rectified output current ($i_{\rm s}$) is controlled as a dc current ($I_{\rm s}$) and $\alpha_{\rm f}$ is the firing angle.

is enhanced by the use of Power Factor Correction (PFC) circuits. Fig. 2 shows the schematic of a PFC-based multi-drive system, where dc-dc boost converters are adopted in the dc-links. In contrast to the ac-dc configuration in Fig. 1, the ac-dc and dc-dc configuration enables modulating the rectified currents (i.e., $i_{\rm s}$ and $i_{\rm d}$), as highlighted in Fig. 2(b). In this way, the currents drawn by the rectifiers can be "controlled" [22], [29], which possibly leads to improved current and power quality. Furthermore, in the case of multi-drive systems as demonstrated in Figs. 1 and 2, by shifting the SCR currents, the quality of the total grid current (e.g., $i_{\rm ga}$) can be enhanced in terms of a lower THD [22], [30]–[32]. In particular, when the rectified output currents ($i_{\rm s}$ and $i_{\rm d}$) are controlled according to Fig. 2(b) as purely dc currents at the same level, the total grid currents will become multi-level, leading to a better THD. However, the effectiveness of the phase-shifted current control is significantly dependent on the total number of parallel drives and the loading conditions of these drive units, which may draw unequal currents (in terms of amplitude) from the grid. Moreover, in practice, it is almost impossible always to ensure that all the drive units are operating at the same loading conditions. As a result, the harmonic mitigation enabled by the phase-shifted current control is degraded.

To tackle this issue, this paper introduces an enhanced phase-shifted control scheme, which can ensure that each drive unit draws the same amount of currents from the grid during operation. As a result, the quality of the total grid current can be maximized by the phase-shifted current control. Note that the enhanced control requires communication among the parallel drives, where partial loading operation should be possible. The rest of this paper is organized as follows. Firstly, the basics of the phase-shifted current control in multi-drive systems is introduced in § II. Then, the load adaptive control strategy is proposed, followed by the experimental results in § III. It has been confirmed that the enhanced phase-shifted current control is effective for harmonic cancellation in multi-drive systems. Finally, § IV draws the conclusion.

II. Enhanced Phase-Shifted Current Control

A. Harmonic Characteristics of Six-Pulse Rectifiers

In order to develop advanced harmonic mitigation strategies, the harmonic characteristics of six-pulse rectifiers should be analyzed first as following. When the rectified output current (e.g., $i_{\rm s}$ or $i_{\rm d}$ in Fig. 2) is controlled as purely dc denoted as $I_{\rm s}$ or $I_{\rm d}$, the corresponding input currents (i.e., $i_{\rm sabc}$ or $i_{\rm dabc}$) appearing in the grid will be rectangular waveforms [33], as shown in Fig. 3 for a SCR unit. In the case of a DR unit, similar square input currents can be obtained by setting $\alpha_{\rm f} = 0$, where all these rectangular currents should be shifted back by a degree of $\alpha_{\rm f}$ and the rectified voltage of six-pulses (i.e., $v_{\rm d}$) in that case is also indicated in Fig. 3. However, these square currents contain high harmonics that are emitted to the grid.

Nevertheless, the square currents in Fig. 3 can be expressed by summing up all harmonic currents as

$$i_{sp}(t) = \sum_{h}^{\infty} i_{sp}^{h}(t) \tag{1}$$

with h = 1, 2, 3, $\cdots$ being the harmonic order, p = a, b, or c, and i_{sp}^{h} being the h-th order harmonic component of the SCR input current that is obtained through the Fourier analysis as

$$i_{sp}^{h}(t) = a_p^h \cos(h\theta) + b_p^h \sin(h\theta) \tag{2}$$

where $\theta = \omega t$ with ω being the angular grid frequency, a_p^h and b_p^h are the corresponding Fourier coefficients. Since $i_{sp}^{h}(t)$ is half-wave symmetrical, there will be no even harmonics (i.e., $a_p^h = b_p^h = 0$ for even h) [33]. For odd harmonics (i.e., h = 1, 3, 5, $\cdots$), the Fourier coefficients can be obtained by

$$a_p^h = \frac{2}{\pi}\int_0^{\pi} i_{sp}(t)\cos(h\theta)\,d\theta, \quad b_p^h = \frac{2}{\pi}\int_0^{\pi} i_{sp}(t)\sin(h\theta)\,d\theta$$

and further given as

$$\begin{cases} a_p^h = \dfrac{2I_{\rm r}}{h\pi}[-\sin(h\alpha_p) + \sin(h\alpha_p + h\beta)] \\ b_p^h = \dfrac{2I_{\rm r}}{h\pi}[\cos(h\alpha_p) - \cos(h\alpha_p + h\beta)] \end{cases} \tag{3}$$

in which α_p is the phase angle for the phase-p current in respect to $\omega t = 0$ (defined to be zero at the positive zero crossing of the phase-a voltage $v_{\rm aN}$ as shown in Fig. 3), and $\beta = 120°$ is

Post Print

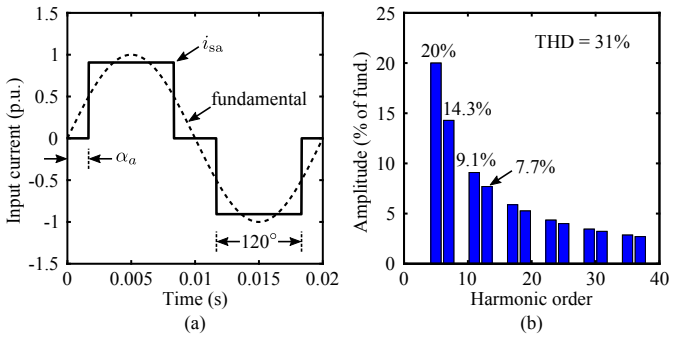

Fig. 4. Harmonic characteristics of the phase-a current drawn by a SCR (or a DR when $\alpha_f = 0$): (a) input current and (b) harmonic distribution.

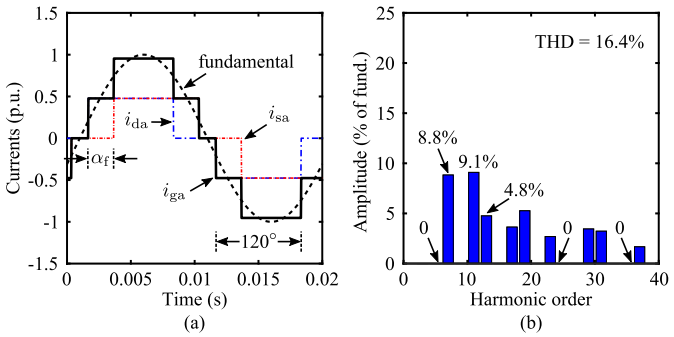

Fig. 5. Harmonic characteristics of the phase-a currents at PCC in a two-drive system (shown in Fig. 2) with the phase-shifted current control, where $\alpha_f = 36°$: (a) typical currents at PCC and (b) harmonic distribution of the total grid current i_{ga}.

the conduction angle. According to Fig. 3, $\alpha_a = \alpha_f + 30°$ for the phase-a current with $\alpha_f \geq 0$ being the SCR firing angle, and thus $\alpha_b = \alpha_a + 120°$ and $\alpha_c = \alpha_a + 240°$.

Furthermore, according to (2) and (3), it is possible to describe the rectangular current waveforms in a compact format. For instance, the phase-a current of the SCR unit (i.e., i_{sa} and $p = a$) can also be given as

$$i_{sa}(t) = \frac{2\sqrt{3}}{\pi} I_s \sum_{k}^{\infty} \left\{ \frac{(-1)^n}{k} \sin[k(\theta - \alpha_f)] \right\} \tag{4}$$

where $k = 6n \pm 1$ is the harmonic order with $k > 0$ and $n = 0, 1, 2, \cdots$. As a consequence, the magnitude (i.e., I_{sa}^k) of the k-th individual harmonic component (represented by $i_{sa}^k(t)$) of the phase-a current can be obtained as

$$I_{sa}^k = \frac{2\sqrt{3}}{k\pi} I_s \tag{5}$$

which can be used to analyze the harmonic characteristics as well as to calculate the current THD:

$$\text{THD}_{i_{sa}} = \frac{1}{I_{sa}^1} \sqrt{\sum_{k \neq 1} \left(I_{sa}^k\right)^2} \times 100 = 31\%. \tag{6}$$

Subsequently, Fig. 4 gives the harmonic distribution of the square currents drawn by a SCR unit, which indicates that the rectangular currents drawn by the SCR or DR contains significant low-order harmonics, leading to a poor THD of around 31%. It should be noted that for both rectifiers such non-triplen low-order harmonic currents are in inverse proportion to the harmonic order (see, (5)), which should be lowered as much as possible in three-phase ASD applications.

B. Phase-Shifted Current Control

As mentioned in the last paragraph, either a SCR-fed or a DR-fed drive system will draw highly distorted currents from the grid. In particular, the low-order harmonic currents (e.g., 5th, 7th, 11th, and 13th) are not desired in such applications, which however can be attenuated to certain levels by a phase-shifted current control in the case of multi-drive systems.

To illustrate this harmonic mitigation strategy, the two-drive system shown in Fig. 2 is adopted in the following, where the h-th harmonic component of the input square currents for the SCR unit can also be represented as a phasor,

$$\mathbf{I}_{sp}^h = I_{sp}^h e^{j\phi_{sp}^h} \tag{7}$$

where I_{sp}^h and ϕ_{sp}^h are the corresponding magnitude and phase, respectively. According to (2) and (3), the magnitude I_{sp}^h and phase ϕ_{sp}^h can be calculated by

$$I_{sp}^h = \left[\left(a_p^h\right)^2 + \left(b_p^h\right)^2 \right]^{1/2} \text{ and } \phi_{sp}^h = \arctan\left(-b_p^h / a_p^h\right) \tag{8}$$

in which, as previously defined, $h = 1, 3, 5, \cdots$ is the harmonic order, a_p^h and b_p^h are the Fourier coefficients of the corresponding phase-p current. In a similar manner, the input rectangular currents i_{dp} for the DR unit can be obtained by substituting $\alpha_f = 0$ into (2) and (3). Hence, the h-th harmonic component of the square currents (i.e., i_{dp}) for the DR unit can also be expressed as phasors by

$$\mathbf{I}_{dp}^h = I_{dp}^h e^{j\phi_{dp}^h} \tag{9}$$

with I_{sp}^h and ϕ_{sp}^h being the corresponding magnitude and phase, respectively, which can be obtained through (3) and (8) considering $\alpha_f = 0$.

According to the superposition principle and Fig. 2, the phasor of the h-th harmonic component of the total currents appearing in the grid (i_{gp}) can be expressed as

$$\mathbf{I}_{gp}^h = \mathbf{I}_{sp}^h + \mathbf{I}_{dp}^h = I_{sp}^h e^{j\phi_{sp}^h} + I_{dp}^h e^{j\phi_{dp}^h} \tag{10}$$

indicating the possibility to cancel out the h-th harmonic component of the total grid current. Specifically, the harmonic cancellation by means of the phase-shifted current control can be attained, only when

$$I_{sp}^h = I_{dp}^h \text{ and } \phi_{sp}^h = \phi_{dp}^h - \pi \tag{11}$$

which will result in $I_{gp}^h = 0$, being the magnitude of the h-th harmonic grid current. Fig. 5 exemplifies the effectiveness of the phase-shifted current control, where the criteria in (11) are accomplished. As a consequence that a phase-shift of 36° has been introduced to the SCR unit, all the harmonics of fivefold the grid fundamental frequency (e.g., the 5th and the 25th harmonics) have been mitigated, leading to an improved THD of around 16.4%.

It should be pointed out that, in practice, there will be more than two drive units connected to the PCC (e.g., in an office building). This further enables the possibility to alleviate the harmonic generation to the grid by means of the

Post-Print

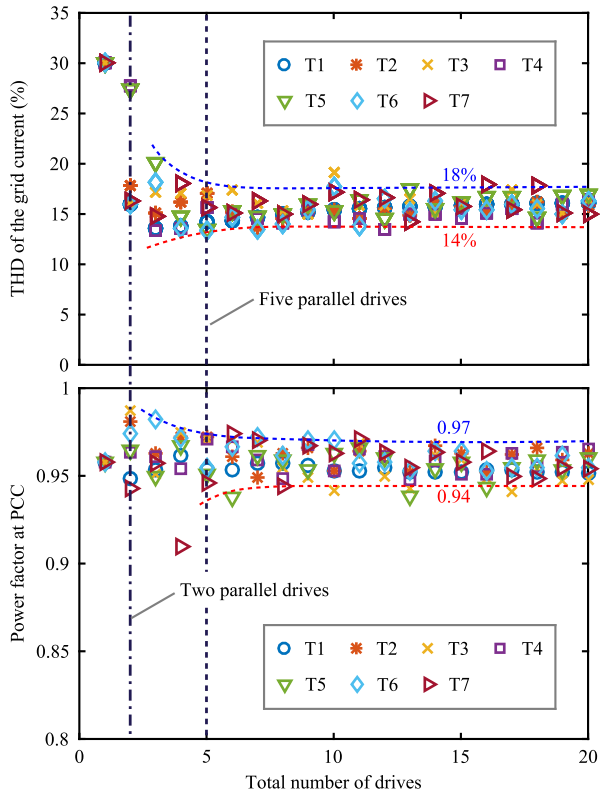

Fig. 6. Simulation results of a multi-drive system considering various number of drives under random loading conditions with linearly-designed firing angles (i.e., $\alpha_{\rm f}^m = (m-1)/(N-1) \times 30$ with m being the drive unit number and N is the total number of drives), where T# represents the case number (for T1, the loading of all drives is equal): (a) THD of the total grid current and (b) power factor at PCC.

phase-shifting control [34], as even more levels of the grid current can be achieved. In that case, the firing angles should be designed specifically in such a manner that the resultant THD of the grid PCC current will become independent of the loading conditions without additional harmonic mitigation devices (e.g., active power filtering systems). It is thus a size- and cost-effective solution for multi-drive systems.

Fig. 6 then presents an example of a multi-drive system (up to 20 drives) under random loading conditions, where the firing angles are linearly assigned within 0° to 30°. It can be observed that, when the total drive number is above five (i.e., $N \geq 5$), both the THD level and power factor tend to be bounded within a narrow bands (i.e., being independent of the loading condition). Specifically, the THD of the grid current will vary within 14% to 18%; the power factor will be around 0.95. However, for a multi-drive system consisting of two drive units, the resultant THD of the grid current will vary in a wide range (15% to 28%). To sum up, unequal loading will affect the harmonic cancellation performance of the phase-shifted control for a small number of parallel drives, which should be addressed properly. The following thus introduces an enhanced phase-shifted control scheme for two-drive systems.

C. Enhanced Phase-Shifted Control Strategy

Clearly, the latter criterion in (11) can be fulfilled by introducing a phase shift to the SCR unit (i.e., $\alpha_{\rm f}$ = 180°/h).

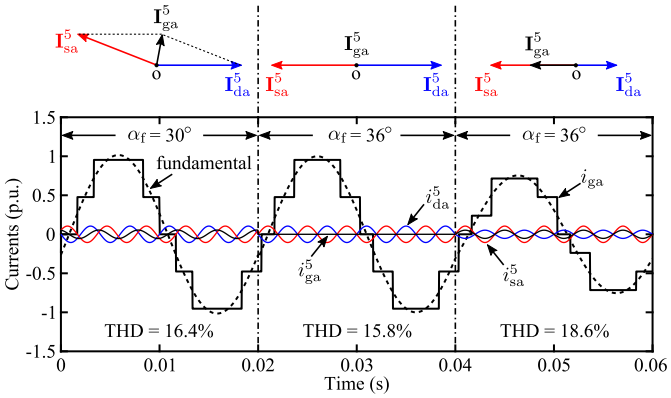

Fig. 7. Illustration of the improper phase-shift and unequal loading (the DR is half-loaded in respect to the loading of the SCR) impacts on the phase-shifted current control for the two-drive system (top: phasors of the 5th harmonics; bottom: typical current waveforms).

However, in practical applications, the loading of the drives is not equal, and thus the magnitudes of the currents drawn by the rectifiers can not be maintained at the same level (i.e., $I_{\rm s}^h \neq I_{\rm d}^h$). Consequently, the performance of the phase-shifted current control is affected, as aforementioned, and it is further illustrated in Fig. 7. It can be observed in Fig. 7 that the THD of the total grid current has been brought to 18.6% in the case of unequal loading between the two drives (the DR is half-loaded in respect to the SCR). Moreover, it is also identified that the THD of the total grid current can be minimized if the loading is equal. Fig. 8 demonstrates that a minimum THD (red dot, 15.8%) of the grid current is achieved, when the rectified output currents are at the same level and $\alpha_{\rm f}$ = 32°. In addition, the impact of unequal loading is further recognized in Fig. 8 as a relationship of both the rectified current level and the phase shift angle. Therefore, in order to maximize the harmonic cancellation effectiveness by the phase-shifted current control, an enhanced scheme is developed in the following, which should ensure that both the rectified output currents of the rectifiers are equal.

It is obvious that the firing angle $\alpha_{\rm f}$ controls the SCR input current phase, and thus the average rectified voltage $\bar{v}_{\rm s}$ that can be given as

$$\bar{v}_{\rm s} = \bar{v}_{\rm d} \cos \alpha_{\rm f} = 1.35 V_{LL} \cos \alpha_{\rm f} \tag{12}$$

in which $\bar{v}_{\rm d}$ is the average rectified voltage of the DR unit and V_{LL} is the Root-Mean-Square (RMS) value of line-to-line grid voltages (e.g., $v_{\rm ab}$). On the condition that communication is available in the multi-drive systems, the loading information can then be obtained. A power ratio γ and a load current ratio λ are then defined as

$$\gamma = \frac{P_{\rm s}}{P_{\rm d}} \text{ and } \lambda = \frac{\bar{i}_{\rm os}}{\bar{i}_{\rm od}} \tag{13}$$

with $P_{\rm s} = \bar{v}_{\rm os} \cdot \bar{i}_{\rm os}$ and $P_{\rm d} = \bar{v}_{\rm od} \cdot \bar{i}_{\rm od}$ being the boost output powers, where $\bar{i}_{\rm os}$ and $\bar{i}_{\rm od}$ are the average load currents (boost converter outputs), and $\bar{v}_{\rm os}$ and $\bar{v}_{\rm od}$ are the average dc-link voltages. Ignoring the power losses on the boost converters gives $P_{\rm s} \approx \bar{v}_{\rm s} \cdot I_{\rm s}$ and $P_{\rm d} \approx \bar{v}_{\rm d} \cdot I_{\rm d}$. Thus,

$$\gamma = \frac{\bar{v}_{\rm os} \cdot \bar{i}_{\rm os}}{\bar{v}_{\rm od} \cdot \bar{i}_{\rm od}} \approx \frac{\bar{v}_{\rm s} \cdot I_{\rm s}}{\bar{v}_{\rm d} \cdot I_{\rm d}} \tag{14}$$

Post-Print

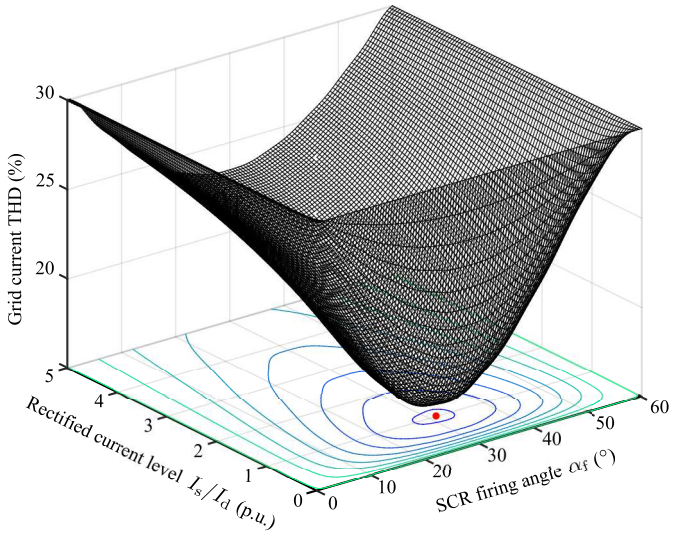

Fig. 8. Performance of the phase-shifted current control for the multi-drive system shown in Fig. 2, when the rectified current level I_s/I_d (defined as current ratio) indicates that the two rectifiers draw different amounts of currents from the grid.

in which I_s and I_d are the average rectified currents shown in Fig. 2 (i.e., controlled as dc currents by the PFC circuits).

As a consequence, in order to maintain the rectified currents at the same level (i.e., $I_s = I_d$), the following condition should be maintained:

$$\frac{\bar{v}_{os}}{\bar{v}_{od}} = \frac{\cos\alpha_f}{\lambda} \tag{15}$$

Hence, if the loading of the drives can be adjusted, the dc-link voltage references v_{od}^* and v_{os}^* for the DR and the SCR unit, respectively, can be set accordingly, which will fulfill the condition in (15). As aforementioned, the communication between the two drive units is required in order to implement (15) in the drive system. It will in return enhance the performance of the phase-shifted current control. Notably, the enhanced phase-shifted control actually "forces" the SCR unit to operate at partial loading in regards to the loading of the DR system:

$$P_s = P_d \cos\alpha_f \tag{16}$$

However, seen from a practical application standpoint, it is almost impossible to achieve the loading of two drives according to (16), although most of the drives are rarely (or not always) operating at rated conditions. Alternatively, in a multi-drive system consisting of several drive units (less than five) with boost converters in the dc-links, certain SCR-fed drive systems can be grouped with the same firing angle according to the loading of the rest drives. In that case, it is still possible to maintain the power relationship of (16). Otherwise, the firing angle should be adjusted according to the loading. Additionally, in a multi-drive system (even more DR-fed and/or SCR-fed ASD systems of unequal loading), the flexibility of power quality maximization can be enhanced, where similar grouping configuration can be applied, thus leading to improved current quality. While in such applications, the firing angles for the SCR drives can also be optimally assigned in order to minimize the harmonic emissions.

TABLE I
PARAMETERS OF THE MULTI-DRIVE SYSTEM (FIG. 2).

Parameter	Symbol	Value
DC-link inductor	L_s, L_d	2 mH
DC-link capacitor	C_s, C_d	470 μF
Grid frequency	f_g	50 Hz
Grid phase voltage (RMS)	$v_{abc,\,N}$	220 V
Grid impedance Z_g	L_g, R_g	0.18 mH, 0.1 Ω
PI dc-link voltage controller	k_p, k_i	0.1, 10

III. RESULTS

In order to verify the effectiveness of the enhanced phase-shifted current control, experiments have been firstly conducted on a two-drive system referring to Fig. 2, where it is assumed that the loading of the drives can be adjusted. The control algorithms are implemented in digital signal processors (Texas Instruments TMS320F28335), where hysteresis and Proportional Integrator (PI) controllers are adopted as the rectified current and dc-link voltage controllers in Fig. 2, respectively (i.e., to control the rectified currents, i_s and i_d, and the output voltages, v_{os} and v_{od}). The PI controller is given in the z-domain as

$$G_{PI}(z) = k_p + \frac{k_i T_s}{2} \cdot \frac{1+z^{-1}}{1-z^{-1}} \tag{17}$$

where k_p and k_i are the proportional and the integral gains, respectively. All the system parameters are listed in Table I.

A. Conventional Phase-Shifted Current Control

Firstly, a firing angle of 32° (i.e., α_f = 32°) is chosen according to Fig. 8 for the minimum THD, where the loading is almost the same (i.e., $\bar{i}_{os} \approx \bar{i}_{od}$). Moreover, v_{os}^* and v_{od}^* are set as 650 V, which means that the enhanced scheme is not enabled although $P_s \approx P_d$. Fig. 9 presents the experimental results for the multi-drive system shown in Fig. 2 with the conventional phase-shifted current control. It can be observed in Fig. 9(c) that the amplitudes of the currents drawn by both rectifiers are not equal (i.e., $I_s \neq I_d$) due to the phase-shifted current control. As a result, the total grid current $\text{THD}_{i_{ga}}$ (i.e., 16.3%) is slightly drifted away from the theoretical minimum value that can be achieved by the phase-shifted current control. This can be even worse when the firing angle is larger and the unequal loading is severer. Nevertheless, with the phase-shifted current control, the grid current quality is improved in contrast to that (31%) shown in Fig. 4.

B. Enhanced Phase-Shifted Control Scheme

Following, the test adopts the enhanced scheme presented in § II, where the dc-link voltages should be set according to (15) and the loading condition (16). That is to say the loading of the drives has been adjusted. For comparison, the firing angle for the SCR remains the same (i.e., α_f = 32°), while the dc-link voltage for the DR unit (i.e., v_{od}^*) has been increased to v_{od}^* = 703 V in order to tolerate the unequal loading (i.e., the unequal rectified currents). The experimental results are shown in Fig. 10.

Post-Print

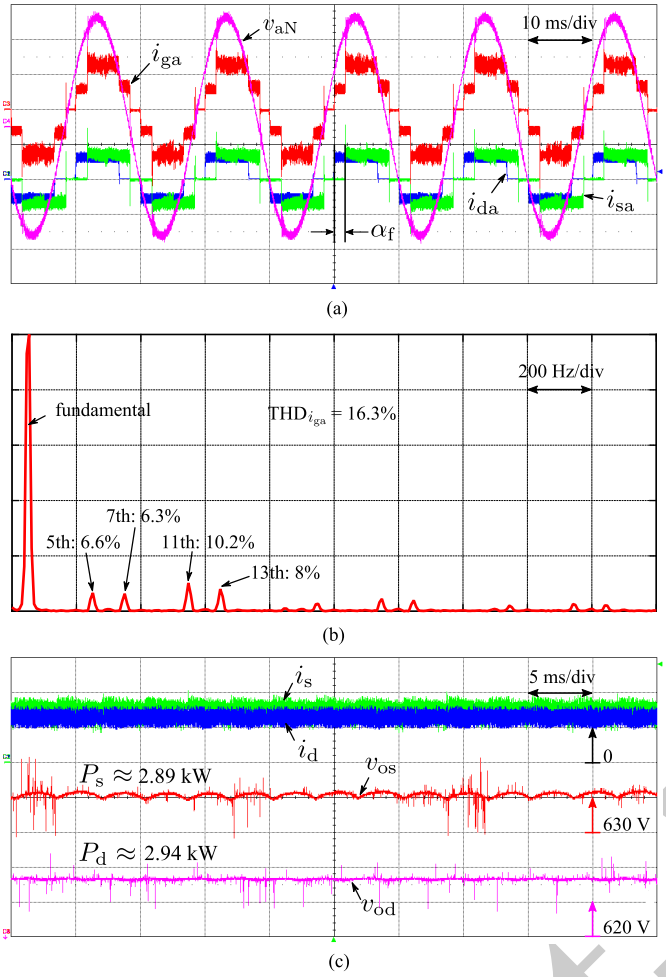

Fig. 9. Experimental results of the multi-drive system shown in Fig. 2 using the phase-shifted current control (α_f = 32°): (a) grid current i_{ga} [10 A/div], grid voltage v_{aN} [200 V/div], DR input current i_{da} [10 A/div], and SCR input current i_{sa} [10 A/div], (b) Fast Fourier Transform (FFT) analysis of the grid current i_{ga} [% of fundamental, 20%/div], and (c) SCR rectified current i_s [5 A/div], DR rectified current i_d [5 A/div], SCR dc-link voltage v_{os} [20 V/div], and DR dc-link voltage v_{od} [20 V/div].

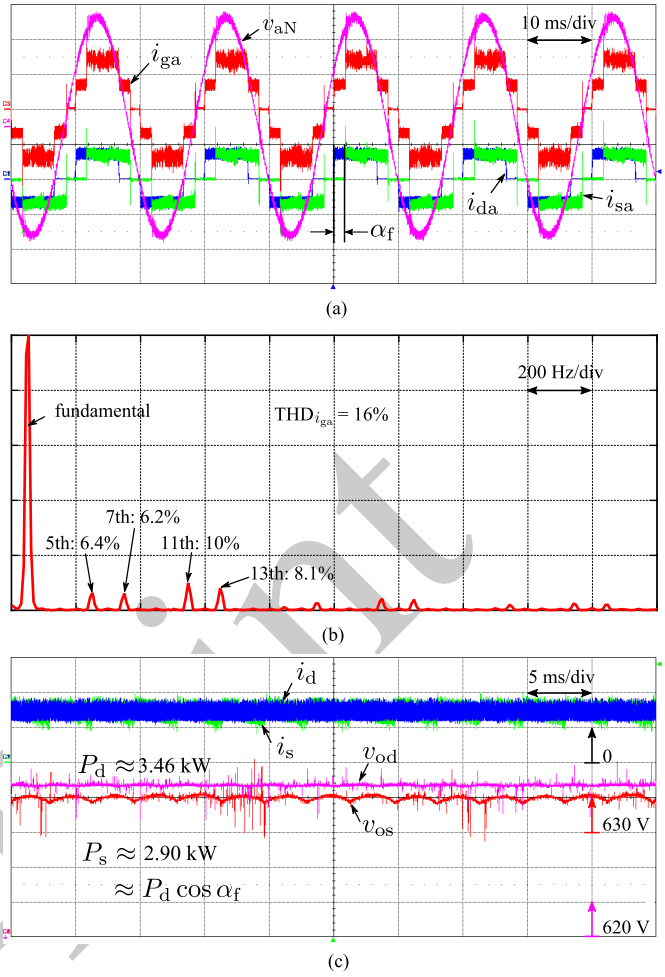

Fig. 10. Experimental results of the multi-drive system shown in Fig. 2 using the enhanced (load adaptive) phase-shifted current control (α_f = 32°): (a) grid current i_{ga} [10 A/div], grid voltage v_{aN} [200 V/div], DR input current i_{da} [10 A/div], and SCR input current i_{sa} [10 A/div], (b) Fast Fourier Transform (FFT) analysis of the grid current i_{ga} [% of fundamental, 20%/div], and (c) SCR rectified current i_s [5 A/div], DR rectified current i_d [5 A/div], SCR dc-link voltage v_{os} [20 V/div], and DR dc-link voltage v_{od} [20 V/div].

Compared to the conventional phase-shifted current control, the proposed control scheme ensures that the rectified currents from both rectifiers are almost at the same level (i.e., $I_s \approx I_d$), as it is shown in Fig. 10(c). Hence, the $THD_{i_{ga}}$ is lowered to 16%, which is close to the theoretical minimum (15.8%). Notably, due to the presence of a grid impedance, it is not possible to achieve the theoretical minimum THD by the phase-shifted control in practice. In addition, it is also indicated in Fig. 10 that, when the enhanced scheme is enabled (implemented), the SCR unit will operate at partial loading condition in respect to the loading of the DR unit (i.e., $P_s \approx P_d \cos \alpha_f$), as what has been assumed. This demonstrates the feasibility to implement the enhanced scheme practically by partially operating certain drives. In all, the above tests are in agreement with the discussions in § II.

In order to further demonstrate the effectiveness of the proposal, more tests have been carried out on the same two-drive system. In this case, the loading of the SCR unit is around 80% of the DR unit when the dc-link voltages are the same. This will lead to unequal input currents for the rectifiers, and thus a poor current quality if the conventional phase-shifted current control is adopted, as previously discussed. Therefore, the enhanced phase-shifted current control scheme is applied to both rectifier units, where the dc-link voltage references are set according to (15) and the firing angle for the SCR is 32° (i.e., α_f = 32°). In particular, the dc-link voltage reference for the DR unit v_{od}^* is reduced to 630 V, while the dc-link voltage reference for the SCR unit remains the same (i.e., v_{os}^* = 650 V). The results are shown in Fig. 11.

As it is shown in Fig. 11(c), the enhanced phase-shifted current control can ensure that the currents drawn by the rectifiers are at the same level. Consequently, the grid current quality is improved (i.e., THD = 16.1%) in contrast to the results with the conventional phase-shifted current control. It should be pointed out that the slight current difference between the rectified currents is induced by the loading variations during operation. All the above experimental tests have demonstrated that the enhanced phase-shifted current

Post-print

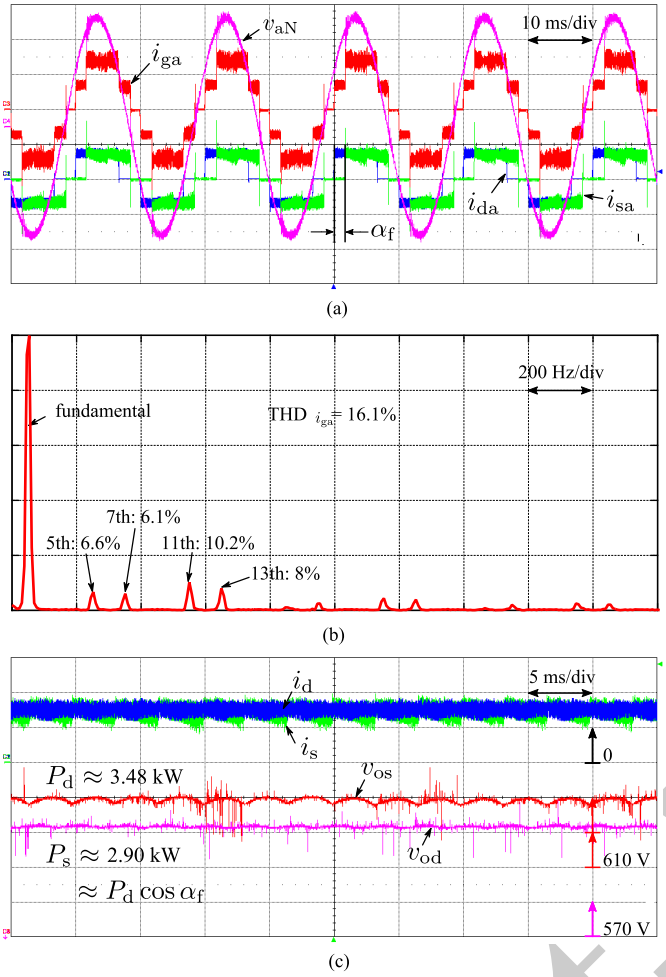

Fig. 11. Experimental results of the multi-drive system shown in Fig. 2 using the enhanced (load adaptive) phase-shifted current control (α_f = 32°) under different power levels: (a) grid current i_{ga} [10 A/div], grid voltage v_{aN} [200 V/div], DR input current i_{da} [10 A/div], and SCR input current i_{sa} [10 A/div], (b) Fast Fourier Transform (FFT) analysis of the grid current i_{ga} [% of fundamental, 20%/div], and (c) SCR rectified current i_s [5 A/div], DR rectified current i_d [5 A/div], SCR dc-link voltage v_{os} [20 V/div], and DR dc-link voltage v_{od} [20 V/div].

control scheme in multi-drive systems can improve the quality of the total currents. While it should be noted that the drive systems may have to operate under different (partial) loading conditions.

C. Case Study on a Four-Drive System

However, practically, it is difficult to operate the drives at the desired power levels. Instead, it is more feasible to consider more drives, where certain drives can be grouped in order to achieve the power relationship in (16). Hereafter, a four-drive system is considered, and Fig. 12 shows the multi-drive system architecture. Compared to the two-drive system shown in Fig. 1, there are two more SCR-fed drives connected to the PCC as shown in Fig. 12, whose parameters are the same as those given in Table I. The nominal power for each drive has been designed at 7.5 kW with the line-to-line voltage being 400 V. Simulations have been carried out in MATLAB/Simulink, where the system has experienced a step-change from a random operation condition to the enhanced

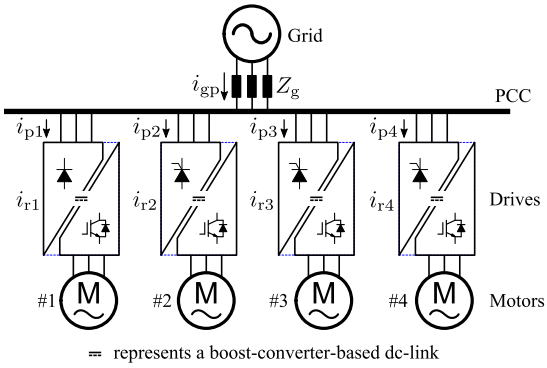

Fig. 12. Architecture of a four-drive system (#1 is a DR-fed drive and #2, #3, and #4 are SCR-fed drives), where i_{gp} is the grid phase current at PCC and i_p represents the current drawn by the corresponding drive with i_r being its rectified current.

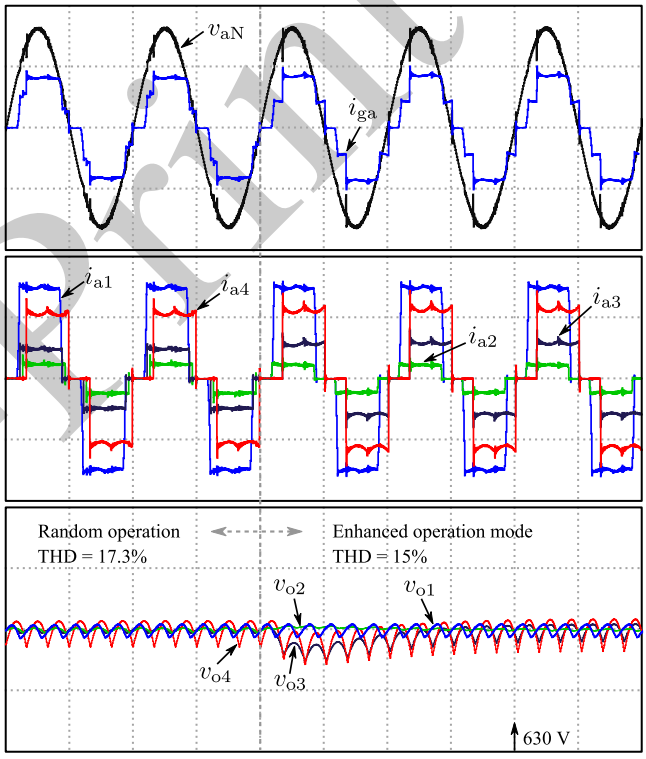

Fig. 13. Simulation results of the four-drive system shown in Fig. 12: grid voltage v_{aN} [200 V/div], grid current i_{ga} [40 A/div], drive input currents (i_{a1}, i_{a2}, i_{a3}, and i_{a4}) [10 A/div], dc-link voltages (v_{o1}, v_{o2}, v_{o3}, and v_{o4}) [10 V/div], and time [10 ms/div].

operation mode (certain drives are grouped). Fig. 13 presents the simulation results.

In the random operation mode, the loading of 7.5 kW, 1.05 kW, 2.38 kW, and 4.34 kW has been recorded, where the corresponding firing angles of 0°, 17.19°, 8.21°, and 26.55° have been observed for the four-drive system (see Fig. 12). As seen in Fig. 13, this random operation results in a THD of 17.3% at the PCC. However, the drives can be grouped according to (16) - #1 and #2 are in one group with the total power being 8.55 kW (denoted as P_1); #3 and #4 are in the other group with the total power being 7.12 kW (denoted as P_2), forming an equivalent "two-drive" system. Thus, when the firing angles are designed as 0°, 0°, 32°, and 32°, it gives

Post-Print

$P_2 \approx P_1 \cos\alpha_f$ with $\alpha_f = 32°$. This meets the condition for the enhanced phase-shifted current control. It is the grouping of drives that leads to a lower THD (15%) of the grid current at the PCC, as shown in Fig. 13, where it can be seen that the multi-drive system can operate stably during the transient. Nevertheless, the above case demonstrates the feasibility of the enhanced scheme in practical multi-drive systems.

IV. Conclusion

In this paper, an enhanced phase-shifted control aiming at harmonic cancellation has been introduced to three-phase multi-drive systems, which have boost converters in the dc-link. The enhancement is achieved by adjusting the drives to operate in partial loading conditions, which in return can ensure that the levels of the currents drawn by the front-end rectifiers are almost equal. Experimental results have confirmed that the enhanced phase-shifted current control can maximize canceling out certain harmonics of interest in the multiple ASD systems by introducing proper phase-shift to the SCR units. That is to say, a minimum THD of the total grid current is almost maintained constant among the parallel drives operating at partial loading conditions. Notably, for practical multi-drive systems consisting of more than two drive units, the harmonic mitigation enabled by the phase-shifted current control can be implemented, as most of the drives are not operating at rated power levels, which has exemplified by simulations. Furthermore, power quality oriented optimization can be performed according to the loading condition.

References

[1] J.W. Kolar and T. Friedli, "The essence of three-phase PFC rectifier systems: Part I," *IEEE Trans. Power Electron.*, vol. 28, no. 1, pp. 176–198, Jan. 2013.

[2] P. K. Steimer, "High power electronics innovation," *presented at ICPE - ECCE Asia*, pp. 1–37, Jun. 2015.

[3] P. Waide and C. U. Brunner, "Energy-efficiency policy opportunities for electric motor-driven systems," 2011.

[4] P. Barbosa, C. Haederli, P. Wikstroem, M. Kauhanen, J. Tolvanen, and A. Savolainen, "Impact of motor drive on energy efficiency," in *Proc. of PCIM*, pp. 1-6, 2007.

[5] S. V. Giannoutsos and S. N. Manias, "A systematic power-quality assessment and harmonic filter design methodology for variable-frequency drive application in marine vessels," *IEEE Trans. Ind. Appl.*, vol. 51, no. 2, pp. 1909–1919, Mar.-Apr. 2015.

[6] F. Zare, "Harmonics issues of three-phase diode rectifiers with a small DC link capacitor," in *Proc. of PEMC*, pp. 912-917, 21-24 Sept. 2014.

[7] W.-J. Lee, Y. Son, and J.-I. Ha, "Single-phase active power filtering method using diode-rectifier-fed motor drive," *IEEE Trans. Ind. Appl.*, vol. 51, no. 3, pp. 2227–2236, May-Jun. 2015.

[8] M. A. S. Masoum and E. F. Fuchs, *Power quality in power systems and electrical machines*. Academic Press, Jul. 2015.

[9] IEC, "Electromagnetic compatibility (EMC) - part 3-2: Limits - limits for harmonic current emissions (equipment input current $\leq$ 16 A per phase)," *IEC/EN 61000-3-2*, 2006.

[10] J. A. Pomilio and G. Spiazzi, "A low-inductance line-frequency commutated rectifier complying with EN 61000-3-2 standards," *IEEE Trans. Power Electron.*, vol. 17, no. 6, pp. 963–970, Nov. 2002.

[11] T. Friedli, M. Hartmann, and J.W. Kolar, "The essence of three-phase PFC rectifier systems: Part II," *IEEE Trans. Power Electron.*, vol. 29, no. 2, pp. 543–560, Feb. 2014.

[12] S. Hansen, P. Nielsen, and F. Blaabjerg, "Harmonic cancellation by mixing nonlinear single-phase and three-phase loads," *IEEE Trans. Ind. Appl.*, vol. 36, no. 1, pp. 152–159, Jan./Feb. 2000.

[13] K. Lee, D. Carnovale, D. Young, D. Ouellette, and J. Zhou, "System harmonic interaction between DC and AC adjustable speed drives and cost effective mitigation," in *Proc. of ECCE*, pp. 4069–4076, Sept. 2015.

[14] H. R. Andersen, R. Tan, and C. Kun, "3-phase AC-drives with passive front-ends with focus on the slim DC-link topology," in *Proc. of PESC*, pp. 3248–3254, Jun. 2008.

[15] F. Meng, W. Yang, Y. Zhu, L. Gao, and S. Yang, "Load adaptability of active harmonic reduction for 12-pulse diode bridge rectifier with active inter-phase reactor," *IEEE Trans. Power Electron.*, vol. 30, no. 12, pp. 7170–7180, Dec. 2015.

[16] S. Choi, P.N. Enjeti, and I.J. Pitel, "Polyphase transformer arrangements with reduced kVA capacities for harmonic current reduction in rectifier-type utility interface," *IEEE Trans. Power Electron.*, vol. 11, no. 5, pp. 680–690, Sept. 1996.

[17] S. Singh and B. Singh, "Optimized passive filter design using modified particle swarm optimization algorithm for a 12-pulse converter-fed LCI - synchronous motor drive," *IEEE Trans. Ind. Appl.*, vol. 50, no. 4, pp. 2681–2689, Jul.-Aug. 2014.

[18] M. M. Swamy, "An electronically isolated 12-pulse autotransformer rectification scheme to improve input power factor and lower harmonic distortion in variable-frequency drives," *IEEE Trans. Ind. Appl.*, vol. 51, no. 5, pp. 3986–3994, Sept.-Oct. 2015.

[19] S. Chiniforoosh, H. Atighechi, and J. Jatskevich, "A generalized methodology for dynamic average modeling of high-pulse-count rectifiers in transient simulation programs," *IEEE Trans. Energy Conversion*, vol. 31, no. 1, pp. 228–239, Mar. 2016.

[20] B. Singh, V. Garg, and G. Bhuvaneswari, "A novel T-connected autotransformer-based 18-pulse AC-DC converter for harmonic mitigation in adjustable-speed induction-motor drives," *IEEE Trans. Ind. Electron.*, vol. 54, no. 5, pp. 2500–2511, Oct. 2007.

[21] H. Akagi and K. Isozaki, "A hybrid active filter for a three-phase 12-pulse diode rectifier used as the front end of a medium-voltage motor drive," *IEEE Trans. Power Electron.*, vol. 27, no. 1, pp. 69–77, Jan. 2012.

[22] Y. Yang, P. Davari, F. Zare, and F. Blaabjerg, "A DC-link modulation scheme with phase-shifted current control for harmonic cancellations in multidrive applications," *IEEE Trans. Power Electron.*, vol. 31, no. 3, pp. 1837–1840, Mar. 2016.

[23] H. Akagi, "Active harmonic filters," *Proceedings of the IEEE*, vol. 93, no. 12, pp. 2128–2141, Dec. 2005.

[24] X. Du, L. Zhou, H. Lu, and H.-M. Tai, "DC link active power filter for three-phase diode rectifier," *IEEE Trans. Ind. Electron.*, vol. 59, no. 3, pp. 1430–1442, Mar. 2012.

[25] P. Xiao, G. K. Venayagamoorthy, and K. A. Corzine, "Seven-level shunt active power filter for high-power drive systems," *IEEE Trans. Power Electron.*, vol. 24, no. 1, pp. 6–13, Jan. 2009.

[26] E. J. Delaney and R. E. Morrison, "Minimisation of interharmonic currents from a current source AC drive by means of a selective DC side active filter," *IEEE Trans. Power Delivery*, vol. 10, no. 3, pp. 1584–1590, Jul. 1995.

[27] H. Akagi and R. Kondo, "A transformerless hybrid active filter using a three-level pulsewidth modulation (PWM) converter for a medium-voltage motor drive," *IEEE Trans. Power Electron.*, vol. 25, no. 6, pp. 1365–1374, Jun. 2010.

[28] M. Rastogi, N. Mohan, and A. Edris, "Hybrid-active filtering of harmonic currents in power systems," *IEEE Trans. Power Delivery*, vol. 10, no. 4, pp. 1994–2000, Oct. 1995.

[29] P. Davari, Y. Yang, F. Zare, and F. Blaabjerg, "A multi-pulse pattern modulation scheme for harmonic mitigation in three-phase multi-motor drives," *IEEE J. Emerg. Sel. Top. Power Electron.*, vol. 4, no. 1, pp. 174–185, Mar. 2016.

[30] F. Zare, "A novel harmonic elimination method for a three-phase diode rectifier with controlled DC link current," in *Proc. of PEMC*, pp. 985-989, 21-24 Sept. 2014.

[31] Y. Yang, P. Davari, F. Zare, and F. Blaabjerg, "Addressing the unbalance loading issue in multi-drive systems with a DC-link modulation scheme for harmonic reduction," in *Proc. of APEC*, pp. 221-228, 20-24 Mar. 2016.

[32] E. P. Wiechmann, R. P. Burgos, and J. R. Rodriguez, "Active front-end optimization using six-pulse rectifiers in multi-motor AC drives applications," in *Proc. of IEEE IAS Annual Meeting*, vol. 2, pp. 1294-1299, Oct.1998.

[33] N. Mohan, T.M. Undeland, and W.P. Robbins, *Power electronics: converters, applications, and design*, 3rd ed. John Wiley & Sons, Inc., Chapter 6 (pp. 138-147), 2007.

[34] Y. Yang, P. Davari, F. Zare, and F. Blaabjerg, "Deliberately dispatched scr firing angles for harmonic mitigation in multiple drive applications without communication," in *Proc. of PEMD*, pp. 1-6, 19-21 Apr. 2016.

Post-Print

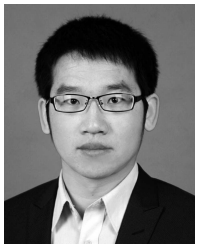

Yongheng Yang (S'12-M'15) received the B.Eng. degree in 2009 from Northwestern Polytechnical University, China and the Ph.D. degree in 2014 from Aalborg University, Denmark.

He was a postgraduate with Southeast University, China, from 2009 to 2011. In 2013, he was a Visiting Scholar with Texas A&M University, USA. Since 2014, he has been with the Department of Energy Technology, Aalborg University, where currently he is an Assistant Professor. His research interests are focused on grid integration of renewable energy systems, power converter design, analysis and control, harmonics identification and mitigation, and reliability in power electronics. Dr. Yang has published more than 80 technical papers and co-authored a book – *Periodic Control of Power Electronic Converters* (London, UK: IET, 2016).

Dr. Yang is a Member of the IEEE Power Electronics Society (PELS) Students and Young Professionals Committee, where he serves as the Global Strategy Chair and responsible for the IEEE PELS Students and Young Professionals Activities. He served as a Guest Associate Editor of IEEE JOURNAL OF EMERGING AND SELECTED TOPICS IN POWER ELECTRONICS, and has also been invited as a Guest Editor of *Applied Sciences*. He is an active reviewer for relevant top-tier journals.

Pooya Davari (S'11-M'13) received the B.Sc. and M.Sc. degrees in electronic engineering from University of Mazandaran (Noushirvani), Babol, Iran, in 2004 and 2008, respectively, and the Ph.D. degree in power electronics from Queensland University of Technology (QUT), Brisbane, Australia, in 2013.

From 2005 to 2010, he was involved in several electronics and power electronics projects as a Development Engineer. During 2010-2014, he designed and developed high-power, high-voltage power electronic systems for multidisciplinary projects such as ultrasound application, exhaust gas emission reduction, and tissue-materials sterilization. From 2013 to 2014 he was with QUT, as a Lecturer. He joined the Department of Energy Technology, Aalborg University, Aalborg, Denmark, as a Postdoctoral Researcher in August 2014, where he is currently an Assistant Professor. His current research interests include active front-end rectifiers, harmonic mitigation in adjustable-speed drives, electromagnetic interference (EMI) in power electronics, high power density power electronics, and pulsed power applications.

Dr. Davari was awarded a research grant from the Danish Council of Independent Research (DFF-FTP) in 2015.

Firuz Zare (S'98-M'01-SM'06) received his PhD in Power Electronics from Queensland University of Technology in Australia in 2002.

He has spent several years in industry as a team leader working on power electronics and power quality projects. Prof. Zare has received several awards such as an Australian Future Fellowship, Symposium Fellowship by the Australian Academy of Technological Science, Early Career Academic Excellence Research Award and John Madsen Medal from Engineers Australia. He has published over 180 journal and conference papers and technical reports in the area of Power Electronics. Prof. Zare is an academic staff at the University of Queensland in Australia and a Task Force Leader of Active Infeed Converters within Working Group one at the IEC standardization TC77A. He is a Senior Member of IEEE, an Associate Editor of IEEE Access journal and the Editor-in-Chief of International Journal of Power Electronics.

Frede Blaabjerg (S'86-M'88-SM'97-F'03) was with ABB-Scandia, Randers, Denmark, from 1987 to 1988. From 1988 to 1992, he was a Ph.D. Student with Aalborg University, Aalborg, Denmark. He became an Assistant Professor in 1992, an Associate Professor in 1996, and a Full Professor of power electronics and drives in 1998 at Aalborg University. His current research interests include power electronics and its applications such as in wind turbines, PV systems, reliability, harmonics and adjustable speed drives.

Prof. Blaabjerg has received 17 IEEE Prize Paper Awards, the IEEE Power Electronics Society (PELS) Distinguished Service Award in 2009, the EPE-PEMC Council Award in 2010, the IEEE William E. Newell Power Electronics Award in 2014 and the Villum Kann Rasmussen Research Award in 2014. He was an Editor-in-Chief of the IEEE TRANSACTIONS ON POWER ELECTRONICS from 2006 to 2012. Prof. Blaabjerg was nominated in 2014 and 2015 by Thomson Reuters to be between the most 250 cited researchers in Engineering in the world.